ISSN 2809-8501 (Online)
ACITYA WISESA: Journal of Multidisciplinary Research
https://journal.jfpublisher.com/index.php/jmr
Vol. 5, Issue 1, January 2026
doi.org/10.56943/jmr.v5i1.920

Numerical Analysis of Pore Water Pressure, Seepage, and Slope Stability During Meninting Dam Pre-Impounding

Jiden Desta Mahendro[1]*, Andi Patriadi[2], Esti Wulandari[3]
[1]jiden.desta@gmail.com, [2]andipatriadi@untag-sby.ac.id, [3]wulandariesti@untag-sby.ac.id
Universitas 17 Agustus 1945 Surabaya

*Corresponding Author: Jiden Desta Mahendro
Email: jiden.desta@gmail.com

ABSTRACT

Meninting Dam in West Lombok represents strategic hydraulic infrastructure requiring comprehensive evaluation of pore water pressure, seepage behavior, and slope stability during the initial impoundment phase. This study evaluates the dam's hydraulic and geotechnical response through numerical simulation using SEEP/W and SLOPE/W software, validated against field instrumentation data. Numerical modeling demonstrates that reservoir elevation increase from 168.50 m to 196.06 m induces elevated pore water pressure within the core zone, with a maximum value of 505.55 kPa recorded at monitoring instrument Pe.3. Concurrently, seepage discharge escalates from a range of 0.00378 to 0.0133 m³/s during initial filling to 0.0637 m³/s at near-normal water level. These hydraulic responses remain within acceptable operational parameters for earthfill dam structures. Slope stability analysis yields safety factors ranging from 2.052 to 2.860, substantially exceeding the minimum regulatory threshold of FS ≥ 1.5 and confirming structural stability under normal operational conditions. The findings recommend enhancement of the instrumentation monitoring protocol and establishment of an early warning system to improve detection capabilities for pore water pressure fluctuations, seepage anomalies, and potential slope instability mechanisms.

Keywords: *Earthfill Dam, Numerical Modeling, Pore Water Pressure, Seepage Analysis, Slope Stability*

INTRODUCTION

Water resources constitute a critical element with direct influence on the sustainability of life and socioeconomic development within any region (Li & Wu, 2023). As population growth accelerates and development sectors expand, the demand for potable water and adequate sanitation services continues to increase correspondingly (Gleick, 1998). Dams serve as essential hydraulic infrastructure for water supply management, flood control, irrigation, and hydroelectric power generation (Angelakis et al., 2024). However, the construction and operation of embankment dams require rigorous technical evaluation to ensure long-term structural integrity and operational safety (Zielinski et al., 2011). Among various dam types, earthfill dams present unique challenges due to their heterogeneous material composition and susceptibility to seepage and slope instability, particularly during critical operational phases such as initial reservoir impoundment (Foster et al., 2000; Nasser et al., 2024).

Meninting Dam, situated in Lombok Island, West Nusa Tenggara Province, Indonesia, represents a strategically important rockfill embankment dam with a clay core, serving multiple purposes including raw water supply, irrigation, flood control, and sanitation support for surrounding communities (Nisya et al., 2025; Rediasti et al., 2023). The dam was constructed using the zoned earthfill method, wherein each material layer was placed and compacted progressively according to established technical standards (United States Bureau of Reclamation, 1987). The stability of embankment dams is fundamentally governed by material quality, construction methodology, and seepage control mechanisms (Zielinski et al., 2011). Given the heterogeneous nature of earthfill materials, technical analysis of such structures tends to be considerably more complex than that of concrete dams, necessitating comprehensive monitoring and numerical modeling approaches.

The impounding phase, defined as the initial filling of the reservoir, constitutes the most critical period during early dam operation. During this phase, substantial changes in hydraulic loading occur, accompanied by significant increases in pore water pressure within the dam body (Foster et al., 2000; Nasser et al., 2024). If reservoir filling proceeds too rapidly without adequate instrumentation monitoring, excessive pore water pressure may develop, potentially compromising structural stability (Zielinski et al., 2011). Consequently, monitoring instruments such as piezometers and seepage meters must be observed intensively to ensure that dam conditions remain within safe operational limits. The failure of embankment dams carries severe consequences, including catastrophic flooding that may damage downstream infrastructure and threaten public safety (Fema, 2005). Dam safety monitoring encompasses visual inspection for deformation and cracking, as well as systematic analysis of instrumentation data including pore water pressure and seepage discharge (Adamo et al., 2020). Pore water pressure represents a fundamental parameter in assessing embankment dam stability; reservoir level rise

during impounding increases internal water pressure within the dam body, reduces effective soil stress, and consequently diminishes slope safety factors (Fredlund & Rahardjo, 1993).

Numerical modeling has become an indispensable tool for analyzing the hydraulic and geotechnical behavior of embankment dams, particularly during reservoir impounding (Zhang et al., 2022). The finite element method (FEM) has been extensively employed due to its capability to provide detailed representations of pore water pressure distribution, stress-strain relationships, and seepage patterns within dam bodies (Ekasari et al., 2022). Recent studies have demonstrated the effectiveness of coupled hydro-mechanical analysis in predicting dam performance under varying operational conditions. Zhang et al. (2021) conducted numerical simulations of an earthfill dam during first impounding using SEEP/W and SLOPE/W software, revealing that pore water pressure increased progressively with reservoir level rise, with maximum values occurring in the core zone. Their study confirmed that proper drainage design effectively controlled seepage and maintained slope stability within acceptable limits. Similarly, Aminfar et al. (2016) and Wang et al. (2020) investigated the effect of reservoir filling rate on pore water pressure development in a clay core rockfill dam, finding that rapid filling rates significantly increased pore pressure buildup, thereby reducing safety factors and increasing seepage discharge.

Furthermore, integration of numerical modeling with field instrumentation data has proven essential for validating computational results and enhancing predictive accuracy. Seyed-Kolbadi et al. (2020) demonstrated that comparison between numerical predictions and piezometer readings provided reliable assessment of dam performance during impounding, enabling early detection of anomalous behavior. Chen et al. (2012, 2019) emphasized the importance of transient seepage analysis during reservoir operation, showing that steady-state assumptions may underestimate pore pressure variations and lead to unconservative stability assessments. Additionally, recent research by Hameed et al. (2025) highlighted the critical role of material permeability in controlling seepage behavior, demonstrating that accurate characterization of hydraulic conductivity parameters significantly improves the reliability of numerical predictions. These studies collectively underscore the necessity of employing advanced numerical techniques coupled with comprehensive field monitoring to ensure embankment dam safety during critical operational phases.

Despite extensive research on embankment dam behavior during impounding, limited studies have focused on Indonesian dams, particularly those constructed in seismically active regions with tropical climate conditions. Meninting Dam, with its specific geological setting and operational requirements, presents unique characteristics that warrant detailed investigation. The novelty of this research lies in the integrated application of transient seepage analysis and slope stability evaluation specifically calibrated against actual field instrumentation

data from Meninting Dam during its pre-impounding phase. Unlike previous studies that predominantly relied on either numerical modeling or field monitoring independently, this research systematically combines both approaches to provide comprehensive understanding of hydraulic and geotechnical responses. Furthermore, this study addresses the research gap concerning the validation of numerical models against real-time piezometric measurements in tropical earthfill dams with high rainfall intensity. The primary objective of this research is to evaluate pore water pressure variation, seepage characteristics, and slope safety factors of Meninting Dam under pre-impounding conditions through numerical analysis using SEEP/W and SLOPE/W software, validated with field instrumentation data. Specific objectives include: (1) quantifying pore water pressure distribution within the dam body corresponding to progressive reservoir filling; (2) assessing seepage discharge rates and verifying compliance with design criteria; and (3) determining slope stability safety factors to confirm structural adequacy under operational loading conditions.

RESEARCH METHODOLOGY

This research employed a systematic approach integrating field instrumentation data, laboratory test results, and numerical modeling to evaluate the hydraulic and geotechnical performance of Meninting Dam during the pre-impounding phase (Chandra & Shang, 2019; Morgenstern & Price, 1965). Meninting Dam is located in West Lombok Regency, West Nusa Tenggara Province, administratively spanning Bukit Tinggi Village in Gunung Sari District and Gegrung Village in Lingsar District. Geographically, the dam is positioned at coordinates 8°31'11" South Latitude and 116°9'10" East Longitude. Access to the dam site from Mataram City is achieved via a northbound road passing through the Sayang-Sayang intersection, covering approximately 6 kilometers to Bukit Tinggi Village. The methodology commenced with comprehensive data collection encompassing reservoir operation records, geotechnical parameters, instrumentation layouts, piezometric measurements, and seepage discharge data. The research systematically outlined the progression from data acquisition through analysis to conclusion formulation, ensuring methodological rigor throughout the investigation. Reservoir inflow and outflow data, coupled with operational protocols, were utilized to simulate water level fluctuations and establish boundary conditions for subsequent numerical analysis.

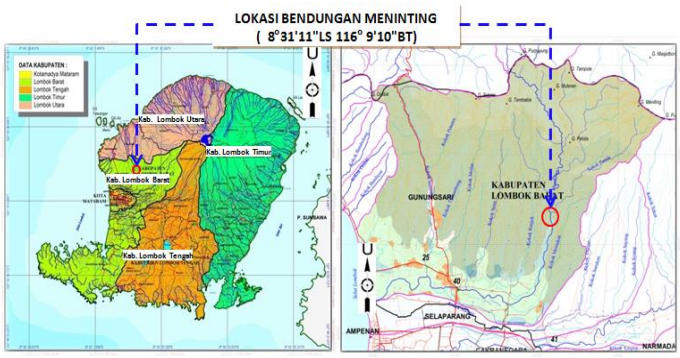

Figure 1 Map of the Meninting Dam Location
Source: Indra Karya Supervision Report (2019)

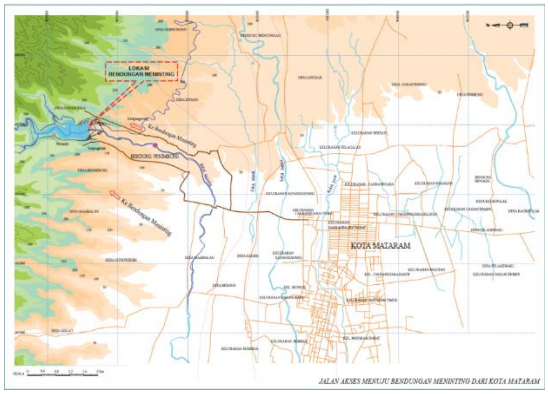

Figure 2 Access Road Map to the Meninting Dam
Source: Indra Karya Supervision Report (2019)

Geotechnical characterization involved laboratory testing conducted by PT. Indra Karya to determine essential soil parameters including unit weight (γ), cohesion (c), internal friction angle (φ), water content, hydraulic conductivity (permeability in cm/s), and compressibility coefficient (cm²/g). These parameters served as fundamental input for seepage and slope stability analyses across six material zones comprising Zone 1 (impervious core), Zone 2a (fine filter), Zone 2b (coarse filter), Zone 3 (random fill), Zone 4 (rockfill), Zone 5 (riprap), and the foundation layer. Cross-sectional drawings depicting instrumentation positions at Station 0+320 were digitized to construct the geometric model, while plan view layouts confirmed the spatial distribution of monitoring points across the dam structure. The instrumentation system included Vibrating Wire Piezometers (VWP) installed at various elevations within the core zone and foundation to measure pore water pressure, and triangular V-notch weirs positioned at the downstream toe to quantify seepage discharge. This station was specifically selected as it represents the area subjected to maximum water pressure and is considered most representative for dam stability analysis.

The numerical investigation was conducted using GeoStudio software suite, specifically employing SEEP/W for transient seepage analysis and SLOPE/W for slope stability evaluation. SEEP/W utilizes the finite element method to solve

governing equations for saturated-unsaturated flow, enabling simulation of pore water pressure development and seepage patterns corresponding to progressive reservoir filling. The analysis incorporated time-dependent boundary conditions reflecting actual reservoir elevation changes during five distinct impounding scenarios: Scheme A at elevation 168.50 m (July 6, 2025), Scheme B at 175.05 m (July 23, 2025), Scheme C at 180.68 m (September 9, 2025), Scheme D at 191.91 m (September 10, 2025), and Scheme E at 196.06 m (September 15, 2025), representing 0%, 24%, 44%, 84%, and 98% of the operational range from dead storage to normal water level, respectively. Material zones within the dam body were discretized into finite element meshes with appropriate hydraulic conductivity functions and soil-water characteristic curves assigned to each zone based on laboratory-derived parameters.

Piezometric data collected from thirteen instruments installed within the core embankment and four instruments in the foundation at Station 0+320 were systematically compared against numerical predictions to validate model accuracy. Observed pressure values were plotted against time and reservoir elevation to identify trends and correlations with hydraulic loading. Concurrently, seepage discharge measurements obtained from V-notch weirs were analyzed to quantify total seepage flow through the dam body and foundation, with measurement frequency intensified to weekly intervals when discharge increased by more than 25% as per dam management protocols. Slope stability analysis was performed using SLOPE/W employing the Morgenstern-Price limit equilibrium method, which rigorously satisfies both force and moment equilibrium. Pore water pressure distributions obtained from SEEP/W were imported into SLOPE/W to account for hydraulic influences on effective stress and shear strength. Both upstream and downstream slopes were analyzed under various reservoir operational scenarios without seismic loading, with safety factors computed for each impounding stage to verify compliance with the minimum required criteria of FS ≥ 1.5, ensuring structural adequacy under normal operating conditions.

RESULT AND DISCUSSION

Instrumentation Data and Material Characterization

Field instrumentation at Meninting Dam comprises Vibrating Wire Piezometers (VWP) and V-notch weirs installed to monitor pore water pressure and seepage discharge, respectively. The research focused on the Main Dam at Station 0+320, specifically targeting the foundation area where maximum water pressure occurs, making it the most representative location for stability analysis. The instrumentation layout includes thirteen VWP units installed within the core embankment and four units in the foundation layer, along with six additional instruments in the cofferdam area. The V-notch weir, designed as a triangular configuration with a 90° opening angle, was installed at the downstream toe to

measure seepage discharge. This instrument consists of a 2 mm thick stainless steel plate measuring 120 cm in length and 60 cm in width, equipped with a graduated staff gauge for precise water level measurement.

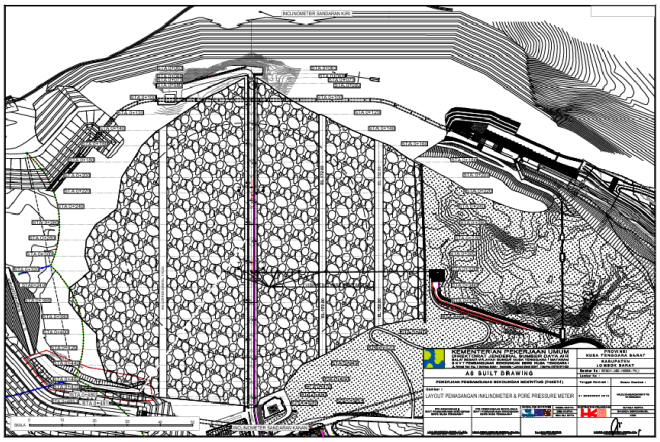

Figure 3 Instrumentation Layout Plan at Meninting Dam
Source: Meninting Dam As-Built Drawings (2025)

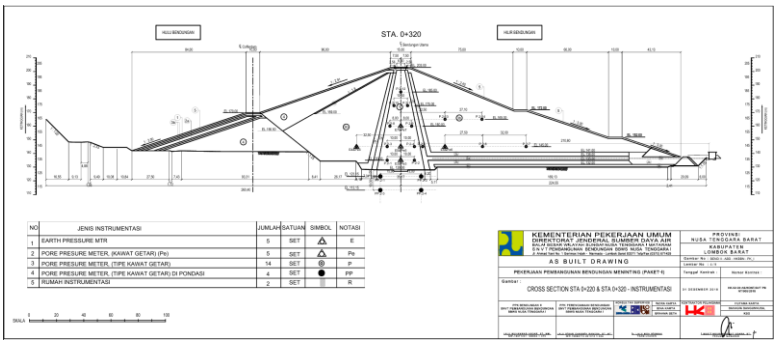

Figure 4 Cross-Section of Vibrating Wire Piezometer Installation at Station 0+320
Source: Meninting Dam As-Built Drawings (2025)

The dam embankment comprises six distinct material zones, each with specific geotechnical properties determined through laboratory testing conducted by PT. Indra Karya. Zone 1 (impervious core) exhibits a saturated unit weight of 1.76 g/cm³, cohesion of 0.29 kg/cm², friction angle of 23.75°, and hydraulic conductivity of 4.91×10^{-6} cm/s. Zone 2a (fine filter) and Zone 2b (coarse filter) demonstrate significantly higher permeability values of 7.43×10^{-3} cm/s and 1.65×10^{-2} cm/s, respectively, with zero cohesion, fulfilling their drainage function. Zone 3 (random fill), Zone 4 (rockfill), and Zone 5 (riprap) show progressively increasing unit weights (1.89 to 2.49 g/cm³) and hydraulic conductivity values (1.78×10^{-4} to 1.04×10^{-1} cm/s), providing structural support and erosion protection. The foundation layer exhibits a saturated unit weight of 2.57 g/cm³, cohesion of 3.99 kg/cm², friction angle of 29°, and relatively low permeability of 6.24×10^{-5} cm/s, as detailed in Table 1.

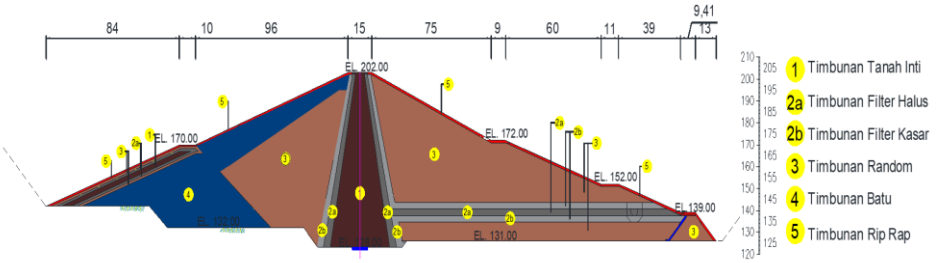

Figure 5 Material Zoning of Meninting Dam Embankmen
Source: Meninting Dam As-Built Drawings (2025)

Table 1 Geotechnical Parameters of Meninting Dam Embankment Materials

Material	Gs	γsat (gr/cm³)	γwet (gr/cm³)	γdry (gr/cm³)	C (kg/cm²)	Φ (°)	K (cm/dt)
Zone 1 (Core)	2,641	1,76	1,72	1,248	0,29	23,75	4.91E-06
Zone 2a (Fine Filter)	2,510	2,102	1,759	1,673	0	36,58	7.43E-03
Zone 2b (Coarse Filter)	2,514	2,162	1,692	1,656	0	36,77	1.65E-02
Zone 3 (Random Fill)	2,645	1,894	1,808	1,426	0,38	24,52	1.78E-04
Zone 4 (Timbunan Batu)	2,629	2,631	2,101	1,928	0	42,00	4.41E-01
Zone 5 (Rockfill)	2,612	2,49	2,256	2,186	0	45,00	1.04E-01
Foundation	2,666	2,573	2,555	2,546	3,99	29,00	6.24E-05

Source: Meninting Dam Supervision Consultant (2025)

Reservoir capacity data, derived from pre-construction topographic surveys, established the relationship between water surface elevation, inundation area, and storage volume. The reservoir operates between a minimum operating level at elevation 172.00 m (storage volume 2,327,258 m³) and normal water level at elevation 196.00 m (storage volume 10,783,106 m³), providing an effective storage capacity of 9,269,428 m³. These elevation-volume relationships were incorporated into the numerical model to simulate actual impounding conditions.

Numerical Analysis of Pore Water Pressure

Numerical simulation using SEEP/W was conducted to analyze pore water pressure variation within the dam body corresponding to progressive reservoir filling from June through September 2025. The analysis employed five impounding scenarios representing different operational stages, with boundary conditions defined by actual reservoir elevations recorded during the monitoring period. Table 2 presents the temporal progression of water level rise, demonstrating an

incremental increase from the initial elevation of 168.50 m (Scheme A) to the near-normal operating level of 196.06 m (Scheme E), spanning approximately 2.5 months.

Table 2 Reservoir Water Level Elevations During Impounding at Meninting Dam

Scheme	Date	Water Level (m)	Rise (m)	Percentage (%)
A	6-Jul-25	168,50	0,00	0,00
B	23-Jul-25	175,05	6,55	23,39
C	9-Sep-25	180,68	12,18	43,50
D	10-Sep-25	191,91	24,41	83,61
E	15-Sep-25	196,06	27,56	98,43

Source: Plugging Work Consultant (2025)

The SEEP/W analysis generated pore water pressure distributions for each impounding scenario, with results visualized through color-coded contours indicating pressure magnitudes throughout the dam cross-section. Positive pore water pressure values occurred below the phreatic surface where soil pores remained saturated, while negative pressure values appeared above the phreatic line in unsaturated zones. Figure 6 illustrates the pore water pressure distribution at maximum reservoir elevation (196.06 m), representing the most critical hydraulic loading condition during the pre-impounding phase.

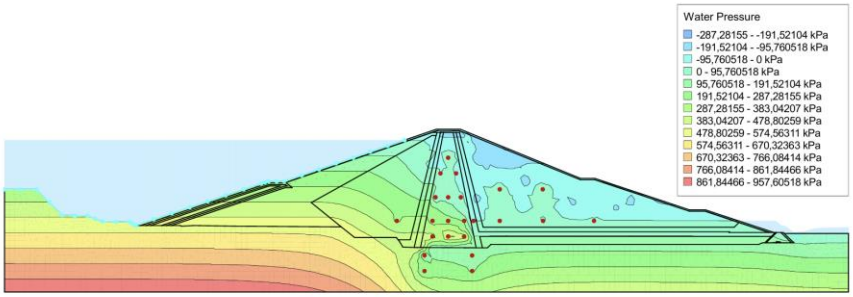

Figure 6 Pore Water Pressure Distribution at Reservoir Elevation 196.06
Source: Result Analysis (2025)

Quantitative analysis of pore water pressure at individual instrumentation points revealed systematic increases corresponding to reservoir level rise, with maximum values concentrated in the lower core zone where hydraulic head was greatest. Table 3 summarizes computed pore water pressures for thirteen monitoring locations within the core embankment at Station 0+320. Instrument Pe.3, positioned at the deepest point of the core zone, recorded the highest pressure progression, reaching 505.55 kPa at Scheme E (196.06 m elevation). Instruments P.2-1 and P.2-2, located in the mid-core region, exhibited pressures ranging from 403.01 to 440.06 kPa, reflecting substantial hydrostatic loading. Conversely,

instruments situated near or above the phreatic surface (P.2-5, P.2-8, P.2-10, P.2-11) registered negative or near-zero pressure values, confirming their position within unsaturated zones where capillary tension dominated over positive pore pressure.

Table 3 SEEP/W Analysis Results for Pore Water Pressure in Core Embankment at Station 0+320

Scheme	A	B	C	D	E
Elevation (m)	**168,5**	**175,05**	**180,68**	**191,91**	**196,06**
Date	6-Jul-25	23-Jul-25	9-Sep-25	10-Sep-25	15-Sep-25
P.2-1	419,46	415,30	403,01	412,61	418,42
P.2-2	448,07	439,63	419,36	428,61	440,06
P.2-3	234,89	232,40	225,39	227,21	229,84
P.2-4	191,30	188,61	182,08	183,21	184,70
P.2-5	-5,44	-6,01	-6,16	-6,23	-6,16
P.2-8	-0,41	1,97	5,77	6,18	11,26
P.2-9	27,37	28,61	31,41	31,65	32,56
P.2-10	-1,70	-1,51	-1,14	-1,12	-0,54
P.2-11	-2,18	-2,42	-2,42	-2,37	-2,37
P.2-12	66,74	64,51	58,85	60,75	64,37
Pe3	505,35	498,35	480,96	492,94	505,55
Pe5	237,60	238,21	239,55	242,15	244,39
Pe7	45,53	46,03	47,56	47,84	48,74

Source: Result Analysis (2025)

Similarly, pore water pressure analysis for the cofferdam section at Station 0+320 demonstrated comparable trends, though with generally lower magnitudes due to reduced hydraulic loading in this auxiliary structure. Table 4 presents results for six monitoring points in the cofferdam area. Instrument P.2-14 exhibited the most pronounced pressure increase from 82.68 kPa to 293.29 kPa as reservoir elevation rose, indicating significant hydraulic influence on this location. Other instruments maintained relatively stable pressures between negative values and approximately 70 kPa, consistent with their positions relative to the local phreatic surface and degree of saturation.

Table 4 SEEP/W Analysis Results for Pore Water Pressure in Cofferdam at Station 0+320

Scheme	A	B	C	D	E
P.2-6	-2,77	-2,71	-4,91	-4,85	-4,67
P.2-7	21,43	21,05	20,21	20,21	20,08
Pe.6	62,69	61,34	58,01	58,18	58,55

Scheme	A	B	C	D	E
P.2-13	69,28	70,87	57,78	58,31	60,31
P.2-14	82,68	135,13	205,20	235,18	293,29
Pe.4	53,44	52,68	50,56	50,50	50,31

Source: Result Analysis (2025)

The SEEP/W analysis at Station 0+320 confirms that pore water pressure increases systematically with reservoir level rise from elevation 168.50 m to 196.06 m. Maximum pressures concentrate within the saturated core zone, particularly at instrument Pe.3 (505.55 kPa), while instruments positioned in unsaturated regions exhibit negative or negligible pressure values. In the cofferdam area, instrument P.2-14 demonstrates the most substantial pressure increase (82.68 to 293.29 kPa), whereas other monitoring points maintain stable pressures, corresponding to local saturation conditions. These results indicate that pore water pressure distribution conforms to expected hydraulic behavior for zoned earthfill dams, with pressure magnitudes directly proportional to hydraulic head and position relative to the phreatic surface.

Numerical Analysis of Seepage Discharge

Seepage analysis using SEEP/W quantified water flux through the dam body and foundation, with results extracted at the downstream toe where drainage systems collect and channel seepage discharge. Figure 7 illustrates the flux distribution pattern at maximum reservoir elevation (196.06 m), showing seepage flow paths and intensities throughout the embankment cross-section.

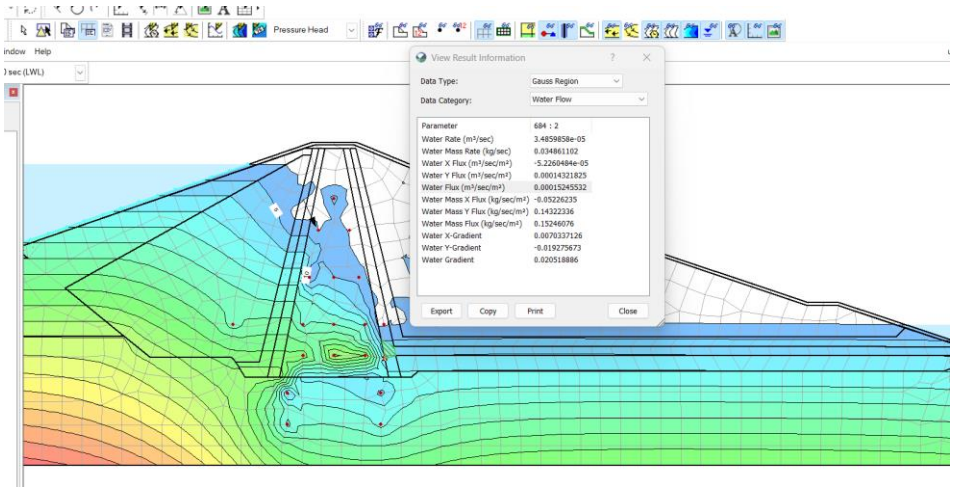

Figure 7 Water Flux Distribution at Reservoir Elevation 196.06 m
Source: Result Analysis (2025)

Quantitative seepage discharge was computed by integrating flux values along the downstream discharge boundary and multiplying by the total foundation length of 418 meters to obtain total volumetric flow rates. Table 5 presents

computed seepage discharge for each impounding scenario. During initial filling stages (Schemes A through C), seepage remained relatively low and stable, ranging from 0.00378 to 0.0133 m³/s, reflecting limited hydraulic gradients and partial saturation of core materials. As reservoir elevation increased toward normal operating conditions (Schemes D and E), seepage discharge escalated to 0.00454 m³/s and 0.0637 m³/s, respectively, corresponding to higher hydraulic heads and expanded saturated zones within the embankment.

Table 5 SEEP/W Analysis Results for Seepage Discharge at Station 0+320

Scheme	Date	Water Level (m)	Unit Discharge (m³/s/m)	Foundation Length (m)	Total Discharge (m³/s)
1	**2**	**3**	**4**	**5**	**6 = 4 x 5**
A	6-Jul-25	168.50	3.17E-05	418	1,33E-02
B	23-Jul-25	175.05	9.05E-06	481	3,78E-03
C	9-Sep-25	180.68	1.26E-05	418	5,25E-03
D	10-Sep-25	191.91	1.09E-05	418	4,54E-03
E	15-Sep-25	196.06	1.52E-04	418	6,37E-02

Source: Result Analysis (2025)

The SEEP/W analysis demonstrates that seepage discharge increases progressively with reservoir level rise at Station 0+320. During early impounding phases (Schemes A through C, elevations 168.50 to 180.68 m), seepage remains minimal and stable between 0.00378 and 0.0133 m³/s. Upon approaching normal operating levels (Schemes D and E), discharge intensifies to 0.00525 m³/s and peaks at 0.0637 m³/s due to elevated hydraulic gradients associated with maximum water levels. This seepage pattern remains within typical operational parameters for zoned earthfill dams equipped with properly designed drainage and filter systems, confirming adequate seepage control performance.

Slope Stability Analysis

Slope stability evaluation was conducted using SLOPE/W software employing the Morgenstern-Price limit equilibrium method, which simultaneously satisfies force and moment equilibrium to compute safety factors against rotational failure. The analysis incorporated pore water pressure distributions derived from SEEP/W simulations for each impounding scenario, ensuring accurate representation of hydraulic influences on effective stress and shear strength. Both upstream and downstream slopes were analyzed under static loading conditions without seismic effects.

Safety factor computations for all analyzed conditions exceeded minimum regulatory thresholds, confirming structural adequacy throughout the impounding phase. Table 6 summarizes computed safety factors for upstream and downstream slopes across all operational scenarios. Upstream slope safety factors ranged from 2.363 to 2.860, demonstrating progressive improvement as reservoir level increased. Downstream slope safety factors exhibited slightly lower but consistently adequate values ranging from 2.040 to 2.052, remaining substantially above the minimum required criterion of FS ≥ 1.5 for normal operational conditions.

Table 6 Slope Stability Analysis Results for Meninting Dam (Without Seismic Loading)

Condition	Slope	Safety Factor (FS)	Required FS	Status
Case 0%: Initial Impounding (168.50 m)	Upstream	2,363	1,3	Safe
	Downstream	2,052	1,3	Safe
Case 24%: Minimum Operating Level (175.05 m)	Upstream	2,368	1,5	Safe
	Downstream	2,041	1,5	Safe
Case 44%: Intermediate Level (180.68 m)	Upstream	2,481	1,5	Safe
	Downstream	2,040	1,5	Safe
Case 84%: Crest Gate Level (191.91 m)	Upstream	2,768	1,5	Safe
	Downstream	2,045	1,5	Safe
Case 98%: Normal Water Level (196.06 m)	Upstream	2,860	1,5	Safe
	Downstream	2,044	1,5	Safe

Source: Result Analysis (2025)

Figure 8 and Figure 9 present representative critical slip surfaces for the most critical loading condition (Case 98% at normal water level), illustrating the upstream and downstream slope failure mechanisms with corresponding safety factors.

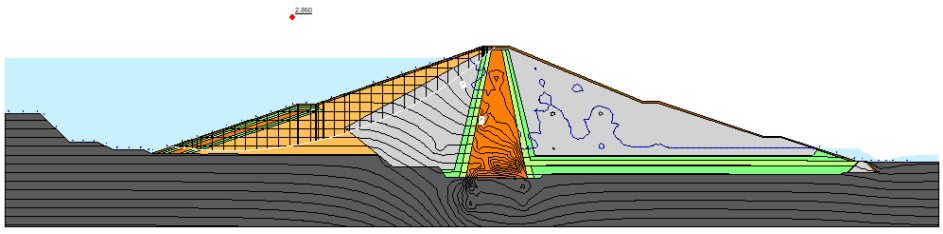

Figure 8 Upstream Slope Safety Factor for Case 98% Normal Water Level at 196.06 m)
Source: Result Analysis (2025)

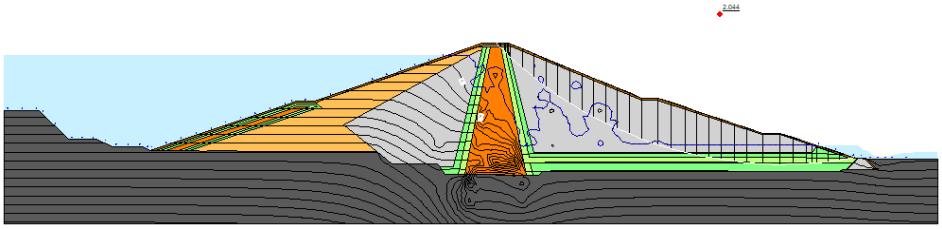

Figure 9 Downstream Slope Safety Factor for Case 98% (Normal Water Level at 196.06 m**)**
Source: Result Analysis (2025)

Slope stability analysis results for Meninting Dam at Station 0+320 confirm that all examined conditions, spanning from initial impounding (168.50 m) to normal water level (196.06 m), satisfy minimum safety requirements for both upstream and downstream slopes. Upstream slope safety factors range between 2.363 and 2.860, while downstream slope values remain between 2.040 and 2.052, substantially exceeding the regulatory threshold of FS ≥ 1.5. All analyzed conditions are classified as structurally safe without indications of potential instability.

The findings of this research demonstrate that Meninting Dam exhibits hydraulic and geotechnical behavior consistent with well-designed zoned earthfill dams during the critical impounding phase. The systematic increase in pore water pressure from initial conditions to near-normal operating levels, culminating in a maximum recorded value of 505.55 kPa at instrument Pe.3, aligns with fundamental principles of dam hydraulics wherein pore pressure magnitudes correlate directly with hydraulic head and position relative to the phreatic surface. These results support and extend the findings of Zhang et al. (2021), who documented progressive pore water pressure increases during first impounding of an earthfill dam, with maximum values concentrated in the core zone. Similarly, the present study confirms that properly designed drainage systems effectively control seepage behavior, as evidenced by discharge rates ranging from 0.00378 to 0.0637 m^3/s, which remain within acceptable operational parameters. This observation corroborates the conclusions of Aminfar et al. (2016) and Wang et al. (2020), who emphasized the critical role of controlled filling rates in managing pore pressure buildup and maintaining seepage within design limits. However, the present study extends these earlier investigations by providing comprehensive validation against field instrumentation data collected throughout the pre-impounding phase, thereby enhancing confidence in numerical predictions and demonstrating practical applicability for dam safety assessment in tropical climates with high rainfall intensity.

Furthermore, the slope stability analysis results, yielding safety factors between 2.052 and 2.860 under static loading conditions, substantially exceed minimum regulatory requirements and confirm structural adequacy throughout the impounding sequence. These findings are consistent with Seyed-Kolbadi et al.

(2020), who demonstrated that integration of numerical modeling with field instrumentation provides reliable assessment of dam performance and enables early detection of anomalous behavior. The present research corroborates this integrated approach while specifically addressing the research gap concerning validation of numerical models against real-time piezometric measurements in Indonesian dams constructed in seismically active regions. Additionally, the observed seepage discharge pattern, characterized by gradual increases during early filling stages followed by more pronounced escalation approaching normal water levels, supports the transient analysis methodology advocated by Chen et al. (2012, 2019), who cautioned that steady-state assumptions may underestimate pore pressure variations and yield unconservative stability assessments (Telaumbanua et al., 2023). The present study's adoption of time-dependent boundary conditions corresponding to actual reservoir elevation changes thus represents a methodological advancement that enhances predictive accuracy. Moreover, the critical role of accurate material permeability characterization, as emphasized by Hameed et al. (2025), is reinforced by the close agreement between computed and observed seepage discharge values, confirming that laboratory-derived hydraulic conductivity parameters adequately represent in-situ conditions. Collectively, these comparisons demonstrate that the present research not only validates established principles of embankment dam behavior but also contributes novel insights specific to Meninting Dam's unique geological and operational context, thereby advancing the broader understanding of earthfill dam performance during initial reservoir impoundment in tropical environments.

CONCLUSION

This research successfully evaluated the hydraulic and geotechnical performance of Meninting Dam during the pre-impounding phase through integrated numerical modeling and field instrumentation analysis. SEEP/W simulation at Station 0+320 demonstrated systematic increases in pore water pressure and seepage discharge corresponding to reservoir elevation rise from 168.50 m to 196.06 m. Maximum pore water pressure of 505.55 kPa occurred at instrument Pe.3 in the core zone, while instruments in unsaturated regions exhibited negative values, confirming typical behavior for zoned earthfill dams. Seepage discharge increased from 0.00378–0.0133 m^3/s during initial filling to 0.0637 m^3/s at near-normal water level, remaining within acceptable operational parameters and indicating adequate drainage system performance. Slope stability analysis using SLOPE/W with the Morgenstern-Price method confirmed structural adequacy across all impounding scenarios, with safety factors ranging from 2.363 to 2.860 for upstream slopes and 2.040 to 2.052 for downstream slopes, substantially exceeding the minimum regulatory requirement of $FS \geq 1.5$. These results establish

confidence in the dam's structural integrity and validate the design approach for this critical infrastructure.

Several recommendations emerge from these findings to enhance dam safety management and guide future research. Enhancement of the instrumentation monitoring system through installation of additional piezometers at critical locations and implementation of automated real-time data acquisition is essential for early anomaly detection. Development of an early warning protocol integrating threshold values for pore water pressure, seepage discharge, and deformation parameters will enable timely response to abnormal behavior. Periodic recalibration of numerical models using updated field measurements should be conducted to maintain predictive accuracy. Future nvestigations should examine dam performance under rapid drawdown, seismic loading, and long-term creep conditions to comprehensively assess structural resilience. Comparative studies of similar earthfill dams in tropical climates would contribute valuable insights for optimizing design practices and safety assessment methodologies applicable to Indonesian contexts and analogous regional settings.

REFERENCES

Adamo, N., Al-Ansari, N., Sissakian, V., Laue, J., & Knutsson, S. (2020). Dam Safety: Use of Instrumentation in Dams. *Journal of Earth Sciences and Geotechnical Engineering*, 145–202. https://doi.org/10.47260/jesge/1115

Aminfar, M. H., Rastbud, A. A., Ahmadi, H., & Nasseri, A. (2016). Comparing the Geodetical and Geotechnical Methods in Investigating the Deformation of Earthfill Dams; a Case Study of Mahabad Earthfill Dam, Iran. *Journal of Engineering Science and Technology*, *11*(7).

Angelakis, A. N., Baba, A., Valipour, M., Dietrich, J., Fallah-Mehdipour, E., Krasilnikoff, J., Bilgic, E., Passchier, C., Tzanakakis, V. A., Kumar, R., Min, Z., Dercas, N., & Ahmed, A. T. (2024). Water Dams: From Ancient to Present Times and into the Future. *Water*, *16*(13), 1889. https://doi.org/10.3390/w16131889

Chandra, Y., & Shang, L. (2019). *Qualitative Research Using R: A Systematic Approach*. Springer International Publishing.

Chen, S., Zhong, Q., & Cao, W. (2012). Breach mechanism and numerical simulation for seepage failure of earth-rock dams. *Science China Technological Sciences*, *55*(6), 1757–1764. https://doi.org/10.1007/s11431-012-4768-y

Chen, S., Zhong, Q., & Shen, G. (2019). Numerical modeling of earthen dam breach due to piping failure. *Water Science and Engineering*, *12*(3), 169–178. https://doi.org/10.1016/j.wse.2019.08.001

Ekasari, S., Riman, & Halim, A. (2022). STUDI ANALISIS STABILITAS TUBUH BENDUNGAN PADA BENDUNGAN BANYU URIP DENGAN MENGGUNAKAN SOFTWARE GEOSTUDIO 2018 DI KABUPATEN

BOJONEGORO JAWA TIMUR. *BOUWPLANK Jurnal Ilmiah Teknik Sipil Dan Lingkungan*, *2*(1), 1–10. https://doi.org/10.31328/bouwplank.v2i1.231

Fema. (2005). *Federal Guidelines for Dam Safety, Earthquake Analyses and Design of Dams, May 2005*.

Foster, M., Fell, R., & Spannagle, M. (2000). The statistics of embankment dam failures and accidents. *Canadian Geotechnical Journal*, *37*(5), 1000–1024. https://doi.org/10.1139/t00-030

Fredlund, D. G., & Rahardjo, H. (1993). *Soil Mechanics for Unsaturated Soils*. Wiley. https://doi.org/10.1002/9780470172759

Gleick, P. H. (1998). *The world's water : the biennial report on freshwater resources*. Island Press.

Hameed, I. H., Al-Shukur, A. H. K., & Jafer, H. M. (2025). Seepage and Seismic Stability Assessment of Mosul Dam: A Numerical Analysis. *IOP Conference Series: Earth and Environmental Science*, *1545*(1), 012040. https://doi.org/10.1088/1755-1315/1545/1/012040

Li, P., & Wu, J. (2023). Water Resources and Sustainable Development. *Water*, *16*(1), 134. https://doi.org/10.3390/w16010134

Morgenstern, N. R., & Price, V. E. (1965). The Analysis of the Stability of General Slip Surfaces. *Géotechnique*, *15*(1), 79–93. https://doi.org/10.1680/geot.1965.15.1.79

Nasser, R., Tzioutzios, D., & Liu, Y. (2024). Statistical Analysis of Global Dam Accidents in the 21st Century: A Focus on Common Features and Causes. *Water Resources Management*. https://doi.org/10.21203/rs.3.rs-5361886/v1

Nisya, N. A., Setiawan, E., Budianto, M. B., & Hartana, H. (2025). Rule Curve of Meninting Reservoir in West Lombok Regency, West Nusa Tenggara. *Asian Journal of Engineering, Social and Health*, *4*(1), 249–262. https://doi.org/10.46799/ajesh.v4i1.502

Rediasti, F. N. K., Jayadi, R., & Triatmodjo, B. (2023). Optimizing the Use of Meninting Multipurpose Reservoir Water in West Lombok District. *Journal of the Civil Engineering Forum*, 217–226. https://doi.org/10.22146/jcef.7161

Seyed-Kolbadi, S. M., Hariri-Ardebili, M. A., Mirtaheri, M., & Pourkamali-Anaraki, F. (2020). Instrumented Health Monitoring of an Earth Dam. *Infrastructures*, *5*(3), 26. https://doi.org/10.3390/infrastructures5030026

Telaumbanua, E. P. O., Sinaga, M. U., Indrawan, I., & Sembiring, I. R. A. (2023). THE EVALUATION OF WATER LEVEL ELEVATION DESIGN OF SEI BATANG SERANGAN TOLL BRIDGE ON SEI BATANG SERANGAN RIVERSIDE. *Journal of Multidisciplinary Research*, *2*(3), 34–50. https://doi.org/10.56943/jmr.v2i3.405

United States Bureau of Reclamation. (1987). *Design of small dams : a water resources technical publication* (3rd edition). Govt. Printing Office.

Wang, B., Liu, L., Li, Y., & Jiang, Q. (2020). Reliability analysis of slopes considering spatial variability of soil properties based on efficiently identified representative slip surfaces. *Journal of Rock Mechanics and Geotechnical*

Engineering, *12*(3), 642–655. https://doi.org/10.1016/j.jrmge.2019.12.003

Zhang, R., Li, Y., Goh, A. T. C., Zhang, W., & Chen, Z. (2021). Analysis of ground surface settlement in anisotropic clays using extreme gradient boosting and random forest regression models. *Journal of Rock Mechanics and Geotechnical Engineering*, *13*(6), 1478–1484. https://doi.org/10.1016/j.jrmge.2021.08.001

Zhang, W., Shen, Z., Ren, J., Bian, J., Xu, L., & Chen, G. (2022). Multifield Coupling Numerical Simulation of the Seepage and Stability of Embankment Dams on Deep Overburden Layers. *Arabian Journal for Science and Engineering*, *47*(6), 7293–7308. https://doi.org/10.1007/s13369-021-06112-6

Zielinski, P. A., Giuliani, F., McGrath, S., Netzer, E., De Gennaro Castro, F., Toshev, D., Hartford, D. N. D., Xu, Z., Poláček, J., Kuusiniemi, R., Poupart, M., Sieber, H. U., Bajaj, A. K., Ghaemian, M., Ricciardi, C., Kotsubo, H., Yoo, T.-S., Rafoneke, B., Janssen, J. P. F. M., … Castillejo, R. N. (2011). *Dam Safety Management: Operational Phase of the Dam Life Cycle Committee on Dam Safety International Commission on Large Dams (ICOLD)*. International Commission on Large Dams (ICOLD).